Distribution Agreement

In presenting this thesis as a partial fulfillment of the requirements for a degree from Emory University, I hereby grant to Emory University and its agents the non-exclusive license to archive, make accessible, and display my thesis in whole or in part in all forms of media, now or hereafter now, including display on the World Wide Web. I understand that I may select some access restrictions as part of the online submission of this thesis. I retain all ownership rights to the copyright of the thesis. I also retain the right to use in future works (such as articles or books) all or part of this thesis.

Kiana Khosravian April 11, 2017

Characterizing a novel transgenic mouse model to investigate α-synuclein-dependent intestinal pathology involved in Parkinson's disease

by

Kiana Khosravian

Dr. Malú G. Tansey
Adviser

Department of Biology

Dr. Malú G. Tansey

Adviser

Dr. Arri Eisen

Committee Member

Dr. David Weinshenker

Committee Member

2017

Characterizing a novel transgenic mouse model to investigate α-synuclein-dependent intestinal pathology involved in Parkinson's disease

By

Kiana Khosravian

Dr. Malú G. Tansey

Adviser

An abstract of
a thesis submitted to the Faculty of Emory College of Arts and Sciences
of Emory University in partial fulfillment
of the requirements of the degree of
Bachelor of Sciences with Honors

Department of Biology

2017

Abstract

Characterizing a novel transgenic mouse model to investigate α-synuclein-dependent intestinal pathology involved in Parkinson's disease

By Kiana Khosravian

Motor deficits are the clinical hallmark of Parkinson's disease (PD), and are the direct result of degeneration of dopaminergic neurons. This degeneration is thought to be caused by aggregated alpha-synuclein found in Lewy bodies in the locus coeruleus, substantia nigra pars compacta (SNpc), and other brain regions [1]. More recent studies have shown that alpha-synuclein aggregates can be found in the gastrointestinal system of PD patients before motor symptoms begin, suggesting there could be a temporal and anatomical link between synuclein aggregation in the gut and the brain in PD [2]. Currently there is not an accurate rodent model that could be used to study how aggregated alpha-synuclein in the gut may contribute to alpha-synuclein aggregation in the brain [3]. Most rodent models address and focus on certain features of the disease but do not recapitulate all aspects of the disease, and few recapitulate gut pathology.

Our laboratory has developed a new mouse model to investigate the role of alpha-synuclein aggregation in degeneration of the noradrenergic system in PD and its relationship to dopaminergic neurodegeneration. In this transgenic mouse model, neurons express wild-type human alpha-synuclein under the control of the dopamine beta-hydroxylase (DBH) promoter, the rate-limiting enzyme in synthesis of norepinephrine. We expect to see human alpha-synuclein expression, phosphorylation, and aggregation, not only in the LC of the transgenic mouse model, but also in the noradrenergic terminals of the gut. We predict that aggregated human alpha-synuclein in the gut will lead to intestinal inflammation, which may promote propagation of alpha-synuclein from the gut to the central nervous system via the vagus nerve or dorsal motor nucleus (DMN) of X. For this thesis project, I confirmed that the human alpha-synuclein

transgene in the bacterial artificial chromosome (BAC) under the control of the DBH promoter and regulatory elements was being transcribed into mRNA and translated into protein in the small intestine and colon of transgenic mice with age-dependent accumulation. I also confirmed co-localization of human alpha-synuclein to enteric neurons through immunofluorescence, and I also found differences in levels of the cytokines interleukin-6 (IL-6) and transforming growth factor beta 1 (TGFβ) between transgenic and non-transgenic mice indicative of preliminary inflammation.

Characterizing a novel transgenic mouse model to investigate α-synuclein-dependent intestinal pathology involved in Parkinson's disease

By

Kiana Khosravian

Dr. Malú G. Tansey

Adviser

A thesis submitted to the Faculty of Emory College of Arts and Sciences
of Emory University in partial fulfillment
of the requirements of the degree of
Bachelor of Sciences with Honors

Department of Biology

2017

Acknowledgements

First, I would like to extend my sincerest gratitude to Dr. Malú Tansey for giving me the opportunity to work in her lab for the past two years, and constantly challenging me to be a better student, scientist and active citizen, and for providing me with priceless mentorship and many life-changing opportunities. I would also like to thank my graduate student mentor, Madelyn Houser, who taught me most of the laboratory practices I know today, and instilled in me values and disciple that made me a better scientist. I would like to acknowledge the entire Tansey lab for their patience, encouragement and constructive feedback.

Additionally, I would like to thank the members of the Tansey, Weinshenker, Miller and Caudle laboratories for their useful discussions and technical assistance.

I would also like to thank my honors committee members, Dr. Malú Tansey, Dr. David Weinshenker, and Dr. Arri Eisen for their support and invested time in the thesis-defending process.

I would also like to acknowledge the fellowships that helped support my research and I through the summer. This work was supported by PDF-APDA Summer Student Fellowship (PDF-APDA-SFW-1672), and the APS UGSRF Fellowship.

Lastly, I would like to thank Emory University and Oxford College of Emory University for valuing the importance of a liberal arts education and the role that independent undergraduate research plays in furthering one's education past the classroom.

Table of Contents

Introduction:

Parkinson's disease (PD) is the second most common neurodegenerative disorder, with over 200,000 new cases per year [4, 5]. PD affects more men than women and manifest on average around age 60. About 90% of PD cases are idiopathic, and only 30% of inherited cases are caused by known monogenic mutations [6]. PD is diagnosed based on the presence of characteristic motor symptoms, a combination of bradykinesia, rigidity, resting tremor, and freezing of gait [7]. The neurohistological hallmark of PD is the degeneration and loss of dopaminergic neurons. This degeneration is thought to be caused at least in part by aggregated alpha-synuclein (αSYN) protein found in Lewy bodies in the locus coeruleus (LC), substantia nigra pars compacta (SNpc), and other brain regions [8]. However, multiple studies have now shown that there is much more to PD than the degeneration of dopamine neurons happening in the brain [2, 9-13].

In addition to motor symptoms, PD is also characterized by non-motor symptoms, some of which can precede motor impairments. The most common non-motor symptoms include hyposmia, constipation, anxiety, rapid eye movement sleep behavior disorder, depression, excessive daytime sleepiness, impaired reaction time, and impaired executive function [9, 14]. Hyposmia and constipation are the most prevalent non-motor symptoms and appear in about 50-75% of cases [9]. Constipation is due to a prolonged intestinal transit time; transit time is controlled by the enteric nervous system [10, 11, 15].

Studies have shown that αSYN is present in the enteric nervous system of healthy control patients, but that it is detected more frequently and at higher levels in the intestines of PD patients [1, 7, 12, 13, 16, 17]. Phosphorylated and aggregated αSYN have also been found in the

stomach, small intestine, colon, and rectum of PD patients [18, 19] . Gastric αSYN inclusions have been implicated in brain pathology in PD patients [1].

The most direct anatomical link between the gut and the brain is the vagus nerve. The vagus nerve is responsible for the main parasympathetic innervation of the stomach, small intestine, and appendix, and terminates before the distal colon [20]. It has been proposed that the vagus nerve can serve as a direct conduit by which phosphorylated and aggregated αSYN from the intestine can pass to the brain [21, 22].

We and others have proposed a working model to explain the role of the gut in PD pathogenesis involving inflammation that is triggered in the gut resulting in chronic low-level inflammation peripherally. This inflammation would in turn increase αSYN in the gut, which in turn would further aggravate inflammation [23-25]. Excess αSYN in the gut, could then travel from the gut to the brain via the vagus nerve. The pathology of PD in the central nervous system (CNS) then starts in the dorsal motor nucleus (DMN) and spreads throughout the brain, eventually reaching the LC, SNpc, and then higher cortical areas [1].

Currently there are no adequate mouse models that recapitulate the aggregated alpha-synuclein present both in the gut and in the brain of PD patients [3]. Most models address and focus on certain aspects of the disease but do not recapitulate most features of the disease as it occurs in humans. One of the earliest and most common forms of modeling PD in rodents was to use the oxidative neurotoxin 6-hydroxydopamine (6-OHDA) to kill dopaminergic neurons. While the 6-OHDA model faithfully reproduced the loss of dopaminergic neurons and terminals that occur in PD, the degeneration of the LC with depletion of norepinephrine was not replicated. Another, important difference was that the 6-OHDA model failed to develop Lewy bodies or display aggregated αSYN. Two other common neurotoxin used to replicate PD in rodents are 1-

methyl-4-phenyl-1,2,3,6-tetrahydropyridine (MPTP) and rotenone. These models also have limitations, including the lack of αSYN aggregation and Lewy body formation, and there is great variability and differences in sensitivity among rodent species and strains [26].

In conjunction with the Weinshenker lab (Emory University, Atlanta, GA), our lab has developed a new transgenic mouse model for PD. In this DBH-hSNCA mouse model, neurons express wild-type human alpha-synuclein (hSNCA) under the control of the dopamine beta-hydroxylase (DBH) promoter. DBH is an enzyme that catalyzes the breakdown of dopamine to norepinephrine [27]. The main advantage of the DBH-hSNCA mouse model is the potential to study the effects of hSNCA expression and aggregation, not only in the LC but also in the gut. The DBH-hSNCA is unique because it expresses wild-type hSNCA. This is significant because 90% of PD cases are idiopathic and patients develop PD although they express wild-type hSNCA. In order to more accurately characterize PD in a mouse model it would be essential to express wild-type hSNCA, because wild-type hSNCA is found in the majority of PD patients.

We hypothesize that the DBH-hSNCA mouse model will more accurately model the proteinopathy of PD in mice by exhibiting aggregated hSNCA, not only in the brain, but also in the gut. We predict that aggregated hSNCA in the gut could potentially lead to intestinal inflammation, which could lead to an increased permeability of the intestine, which can cause systemic inflammation and in turn neuroinflammation.

Successful characterization of this mouse model would enable researchers to study the protein aggregation pathology characteristic of PD in detail. This genetic model could also be a valuable tool to study the effect of different environmental factors known to increase risk for PD (such as pesticides) [28-30] or diminish risk for PD (such as caffeine) [31-34] and analyze their effects on enhancement or amelioration of αSYN pathology. The long-term goal would be to test

different therapeutic interventions in this pre-clinical model of PD prior to advancing them to the clinic.

Material and Methods:

Mice

Wild-type C57Bl/6 mice (Jackson Laboratories, Bar Harbor, ME) were crossbred with founder mice containing the bacterial artificial chromosome (BAC) construct to establish the hemizygous transgenic DBH-hSNCA line. The BAC construct contains all of the regulatory sequences required for expression of the human SNCA gene under the DBH promoter. The BAC construct was developed by Natty Chalermpalanupap in the lab of Dr. David Weinshenker at Emory University (Atlanta, GA, see Figure 1). For the studies outlined in this thesis, we sacrificed cohorts of mice at 4 and 14 months of age. Transgenic (Tg) mice were co-housed with non-transgenic (NTg) mice in the animal facilities at Whitehead Biomedical Research Building (Emory University, Atlanta, GA), under a controlled light-cycle of 12 hours on and 12 hours off. All animal procedures were approved by the Emory Institutional Animal Care and Use Committee (IACUC).

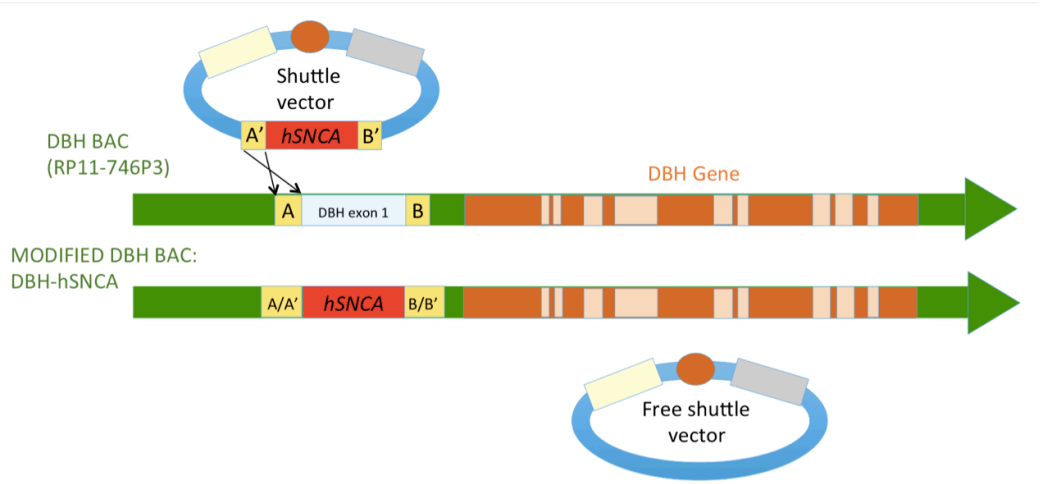

Figure 1: BAC construct containing hSNCA sequence.

Tissue Collection

Mice were anesthetized using isoflurane (Piramal Healthcare, Andhra Pradesh, India) and were subsequently sacrificed using cervical dislocation. Tissue was dissected out and frozen in liquid nitrogen within five minutes of cervical dislocation. Feces and mucous was cleaned from intestinal tissue and the tissue was washed in PBS; 0.5 cm sections of duodenum, jejunum, ileum and colon tissue was collected and flash frozen in liquid nitrogen for later mRNA and protein isolation. The tissue was stored at -80°C until it was processed. The remaining sections of intestinal tissue were cut from proximal to distal end, laid out flat and rolled into Swiss Rolls. The Swiss rolls were fixed in 4% paraformaldehyde (PFA) overnight and then paraffin embedded.

mRNA and Protein Isolation and Quantification

Protein and mRNA were isolated from one-centimeter tissue sections of small intestine and colon tissue. Tissue sections were placed in separate tubes with cold TRIzol Reagent (Ambion by Life Technologies, Carlsbad, CA) and one five-millimeter stainless steel bead (Qiagen, Germany). Samples were placed in a TissueLyser II (Qiagen, German) for dissociation two times for 2 minutes at 20Hz. Samples were pelleted, and the supernatant was transferred to a new tube. One-fifth volume of chloroform was added. Tubes were shaken for 15 seconds and incubated at room temperature for 2 minutes. Samples were then centrifuged, and the upper aqueous phase was transferred to a Qiashredder tube (Qiagen, Germany), centrifuged, and 70% ethanol was added to the flow-through. The lower organic phase was saved for protein isolation. The flow-through was transferred to an RNeasy spin column (Qiagen, Germany), and RNA was extracted according to the manufacturer's protocol. RNA was eluted in 50µl of RNase free water (Qiagen, Germany). Cold methanol was added to the organic phase. Samples were vortexed,

incubated at room temperature for 10 minutes and centrifuged. The supernatant was removed and the pellet was washed with cold methanol and centrifuged again. The pellet was then resuspended in 300µl of radioimmunoprecipitation assay (RIPA) buffer (150mM sodium chloride, 1%Triton X-100 [Sigma, St. Louis, MO] 1% sodium dodecyl sulfate, 50mM Tris hydrochloride, pH 8) using a pestle motor mixer (Argos Technologies, Elgin, IL). Protein concentration was determined using a Pierce BCA Protein Assay Kit (Thermo Scientific, Rockford, IL) according to the manufacturer's protocol.

qPCR

The concentration of RNA was determined using a NanoDrop 2000 Spectrophotometer (Thermo Scientific, Waltham, MA). Four micrograms of RNA were aliquoted into a microfuge tube for cDNA synthesis. One-fifth DNAse I stock was made using a 35:5:10 ratio by volume of UltraPure Distilled Water (Thermo Fischer Scientific, 10977015, Carlsbad, CA), 10X PCR Buffer (Thermo Fischer Scientific, 18067017, Carlsbad, CA), and DNAse I (Thermo Fischer Scientific, 18068-015, Carlsbad, CA). A DNAse Master Mix was prepared using a 3.36:0.64 ratio by volume of 25mM magnesium chloride and 1/5 DNAse I stock and added to the RNA samples. The samples were run on the peqSTAR thermal cycler (VWR, Radnor, PA) at 37°C for 30 minutes, 75°C for 10 minutes. Samples of RNA were then reverse transcribed (RT) to make cDNA. A RT Master Mix was prepared using a 20:10:20:10:1:20 ratio by volume of 5X First Strand Buffer (Thermo Fischer Scientific, 18080093, Carlsbad, CA), 100mM DTT (Thermo Fischer Scientific, y00147, Canada), 10mM of dNTPs (1:1:1:1 ratio of dATP, dTTP, dGTP, dCTP (Thermo Fischer Scientific, 100004916, 18255-018, 18254-011, 18253-013, Carlsbad, CA), 0.8µg/µL Random Hexamers (Integrated DNA Technologies, 5'-NNN NNN-3', Coralville, IA), 200U/µL SuperScript II Reverse Transcriptase (Thermo Fischer Scientific, 100004925,

Carlsbad, CA) and UltraPure Distilled Water. The RT Master Mix was added to the samples and run on the peqSTAR thermal cycler as follows: 25°C for 10 minutes, 42°C for 50 minutes, 72°C for 10 minutes. Distilled water was added to the samples to bring the concentration to 0.02 µg/µl of cDNA. Forward and reverse primers (Integrated DNA Technologies, Coralville, IA) (Table 1) were diluted in UlltraPure Distilled Water to 1.25µM. A qPCR master mix was prepared using a 10.2:20:4.8 ratio by volume of UltraPure Distilled Water, Power SYBR Green PCR Maser Mix (Applied BioSystems, 4367659, Warrington, UK), and the diluted primers. Samples (0.1µg of cDNA) were treated with the qPCR Master Mix, and samples were loaded onto the plate in triplicate. The plate was read on the 7900HT Fast Real-time PCR System (Applied BioSystems, Foster City, CA) and analyzed using SDS 2.3 software (Applied BioSystems, Foster City, CA). Cycle threshold (Ct) values were then averaged from the triplicate results. The averaged Ct values of target genes were then normalized to the average Ct values of two housekeeping genes, Gapdh and cyclophilin F. The normalized Ct values were then subtracted from the same arbitrary number (15) to determine the relative expression values. All subsequent runs were normalized to the original run. The relative expression values per mouse from young (4-month-old) and aged (14-month-old) Tg mice were compared to young and aged NTg mice using a two-way ANOVA and Tukey's multiple comparisons test (GraphPad Prism 6).

Target	Forward Sequence (5' → 3')	Reverse Sequence (5' → 3')
Glyceraldehyde-3-phosphate dehydrogenase (Gapdh)	CAA GGT CAT CCA TGA CAA CTT TG	GGC CAT CCA CAG TCT TCT GG
Peptidylprolyl isomerase F (Cyclophilin F)	TGG AGA GCA CCA AGA CAG ACA	TGC CGG AGT CGA CAA TGA T
Human alpha synuclein (hSNCA)	CAG GAA GGA ATT CTG GAA GAT	TAG TCT TGA TAC CCT TCC TCA

Mouse and human alpha synuclein	AAA TGT TGG AGG AGC AGT GG	GAA GGC ATT TCA TAA GCC TCA
Parkinson disease (autosomal recessive, early onset) 7 (DJ1)	GCA GAG GAG ATG GAG ACA GTG A	GCC TGC AAC AGT GAC TTT GAT C
Interleukin 6 (IL-6)	GAG GAT ACC ACT CCC AAC AGA CC	AAG TGC ATC ATC GTT GTT CAT ACA
Transforming growth factor, beta 1 (TGFβ)	GCA GTG GCT GAA CCA AGG A	AGA GCA GTG AGC GCT GAA TC
Interleukin 10 (IL-10)	GGT TGC CAA GCC TTA TCG GA	ACC TGC TCC ACT GCC TTG CT
Tumor necrosis factor (TNF)	CTG AGG TCA ATC TGC CCA AGT AC	CTT CAC AGA GCA ATG ACT CCA AAG
Interleukin 1 beta (IL-1β)	CAA CCA ACA AGT GAT ATT CTC CAT G	GAT CCA CAC TCT CCA GCT GCA

Table 1: Primers used for qPCR

Western Blots

Protein samples were diluted to 2 µg/µL in 2X Laemmli Sample Buffer (BioRad, Hercules, CA) and 30µg of sample and 5µg of protein ladder (GE Healthcare BioSciences, RPN800E, Pittsburgh, PA) were loaded onto a 12% Mini-PROTEAN TGX Precast Gel (BioRad, Hercules, CA). The gel was run in 1X Tris/Glycine/SDS Buffer (BioRad, Hercules, CA) at 100 volts for 1.5 hours. The gel was then transferred onto an Immobilon-P transfer membrane (Merck Millipore Ltd., Tullagreen, Carrigtwohill, Co. Cork) using Mini Trans-Blot Filter Paper (BioRad, Hercules, CA) and 1x Tris/Glycine Buffer (BioRad, Hercules, CA). The transfer was electrophoresed at 100 volts for one hour. The membrane was then fixed in 0.4% PFA for 30 minutes. The membrane was then cut and blocked in Tris-Buffered Saline with Tween (TBST, 0.1% Tween-20 (Sigma-Aldrich, St. Louis, MO) with 5% milk by weight Blotting-Grade Blocker (BioRad, Hercules, CA) for one hour at room temperature on a rocking platform. The

membrane was then incubated in primary antibody (1:5000 Human alpha Synuclein [Invitrogen, LB509, Carlsbad, CA]; 1:1000 β-Actin [Santa Cruz Biotechnology, SC47778, Dallas, TX]) at 4°C overnight on a rocking platform. The membrane was then washed with TBST and incubated in secondary antibody (1:2000 Goat-anti-Mouse HRP, Jackson ImmunoResearch Laboratories INC., 115-036-072, West Grove, PA) in TBST with 5% by weight Blotting-Grade Blocker for one hour at room temperature on a rocking platform. The membranes were then washed with TBST and TBS before developing. Proteins were visualized using peroxide-developing agents with Pico chemiluminescent reagent (Thermo Scientific, 1856136, 1856135, Rockford, IL) and Femto chemiluminescent reagent (Thermo Scientific, 1858023, 1859022, Rockford, IL). Membranes were imaged in a gel documentation system (G:Box, SynGene, Frederick, MD) using GeneSnap software (SynGene, Frederick, MD). Membrane images were then analyzed using Image Studio Lite (Li-Cor, Version 5.0.21) software to quantify signal strength from the bands of interest. The signal strength values of hSNCA were then normalized to those of β-Actin. The normalized hSNCA values per mouse from young and aged Tg mice were compared to young and aged NTg mice using a two-way ANOVA and Tukey's multiple comparisons test (GraphPad Prism 6).

Staining

Swiss rolls of intestine tissue were fixed in 4% paraformaldehyde PFA overnight. Tissue was then embedded in paraffin, and 5μm sections were cut and mounted on slides. Slides were deparaffinized by a 10-minute incubation in xylene substitute (Histo-Clear, National Diagnostics, Atlanta, GA) at 60°C, followed by two more incubations in xylene at room temperature. Slides were then rehydrated through decreasing concentrations of ethanol and washed in distilled water. Slides were immersed in antigen retrieval buffer (10mM sodium citrate [tribasic, dihydrate],

0.05% Tween-20, pH 6) and incubated in a pressure cooker for 10 minutes at 15-20 psi. Slides were then cooled in an ice bath and washed with distilled water. Slides were then immersed in a blocking solution (5% Bovine Serum Albumin [Gemini Bio-Products, Broderick, CA] 0.5% Triton X-100 [Sigma, St. Louis, MO], 3% Normal Goat Serum [Jackson ImmunoResearch, West Grove, Pennsylvania] in PBS) for one hour. Slides were the incubated in primary antibody at 1:1000 (Human Alpha-synuclein [Invitrogen, LB509, Carlsbad, CA]; Tyrosine Hydroxylase [Millipore, AB152, Billerica, MA]) at room temperature for one hour. Slides were then washed in PBS and incubated with secondary antibody at 1:1000 (Goat-anti-Rabbit AF488 [Thermo Fischer Scientific, A-11070, Eugene, OR], Goat-anti-Mouse AF594 [Thermo Fischer Scientific, A-11020, Eugene, OR]) for 30 minutes at room temperature. Coverslips were then mounted on the slides using Fluoro-Gel with 4',6-diamidino-2-phenylindole (DAPI) (Election Microscopy Sciences, 17985-50, Hatfield, PA) Slides were imaged on a confocal microscope (Olympus FV1000 inverted microscope) using acquisition software (Olympus Fluoview v4.2) to obtain Z-stack images.

Behavioral Assays

Marble Burying: Mice were acclimated in the behavioral room for an hour prior to testing. Mice were then placed in individual large plastic containers, which contained bedding and 20 marbles. Mice spent 30 minutes in each container before being placed back in their home cage. At the end of 30 minutes, the number of marbles that were at least two-thirds buried in the bedding was recorded as buried by two observers blinded to genotype. These values were then averaged and graphed. Averaged marble counts per mouse from Tg mice were compared to NTg mice using an unpaired t-test (GraphPad Prism 6).

Open Field Assay: Mice were acclimated in the behavioral room for an hour prior to testing. A 1'x1' open field was created with white wall borders on each side and a camera mounted at the top, and red lights lit the field evenly so that there were no shadows. Mice were placed into the field from the same corner every time and were recorded for 10 minutes per trial. Between every trial, the number of fecal boli was counted and the field was wiped clean with ethanol. Animal activity was analyzed using Ethovision XT (Noldus) software. The amount of time it took to enter the center or the amount of time spent in a particular area per mouse from Tg mice was compared to NTg mice using an unpaired t-test

Intestinal Transit Time

Carmine Red Assay Mice were fasted for an hour before gavage in their home cage. Mice were gavaged with carmine red dye (6% w/v carmine [Sigma, St. Louis, MO], 0.5% w/v methyl cellulose [Sigma-Aldrich, St. Louis, MO] in sterile PBS); male mice received 300µL of dye and females received 200µL based on size and weight. The time from gavage to expulsion of the first solid red fecal pellet was recorded in minutes. The number of minutes per mouse from Tg mice was compared to NTg mice using an unpaired t-test (GraphPad Prism 6).

Water Content & Fecal Boli Mice were placed in separate, clean cages without food or water for an hour. Stool (fecal boli) produced during this hour were collected immediately after expulsion and placed in tubes with tightly fitting lids. The number of fecal boli expelled over 60 minutes was recorded for each mouse. Tubes were weighed to determine the wet stool weight. Tubes were then incubated overnight at 65°C and weighed the next morning to determine the dry stool weight. The water content percentage was calculated as percent change from wet weight to dry weight. The water content percentage and the number of fecal boli per mouse from Tg mice were compared to NTg mice using an unpaired t-test (GraphPad Prism 6).

Results:

We analyzed the mRNA expression of hSNCA in three different transgenic lines of the DBH-hSNCA mouse model. We found higher expression levels of hSNCA mRNA in line 45 and 76 compared to line 52 in Tg mice by qPCR and western blot analysis (Figure 2a,b,c). We decided to proceed with line 45 and 76 for the remaining experiments based on hSNCA expression levels. We did confirm minimal hSNCA protein expression in line 52 by western blot that positively reflected the low hSNCA mRNA expression measured by qPCR (Figure 2d,e).

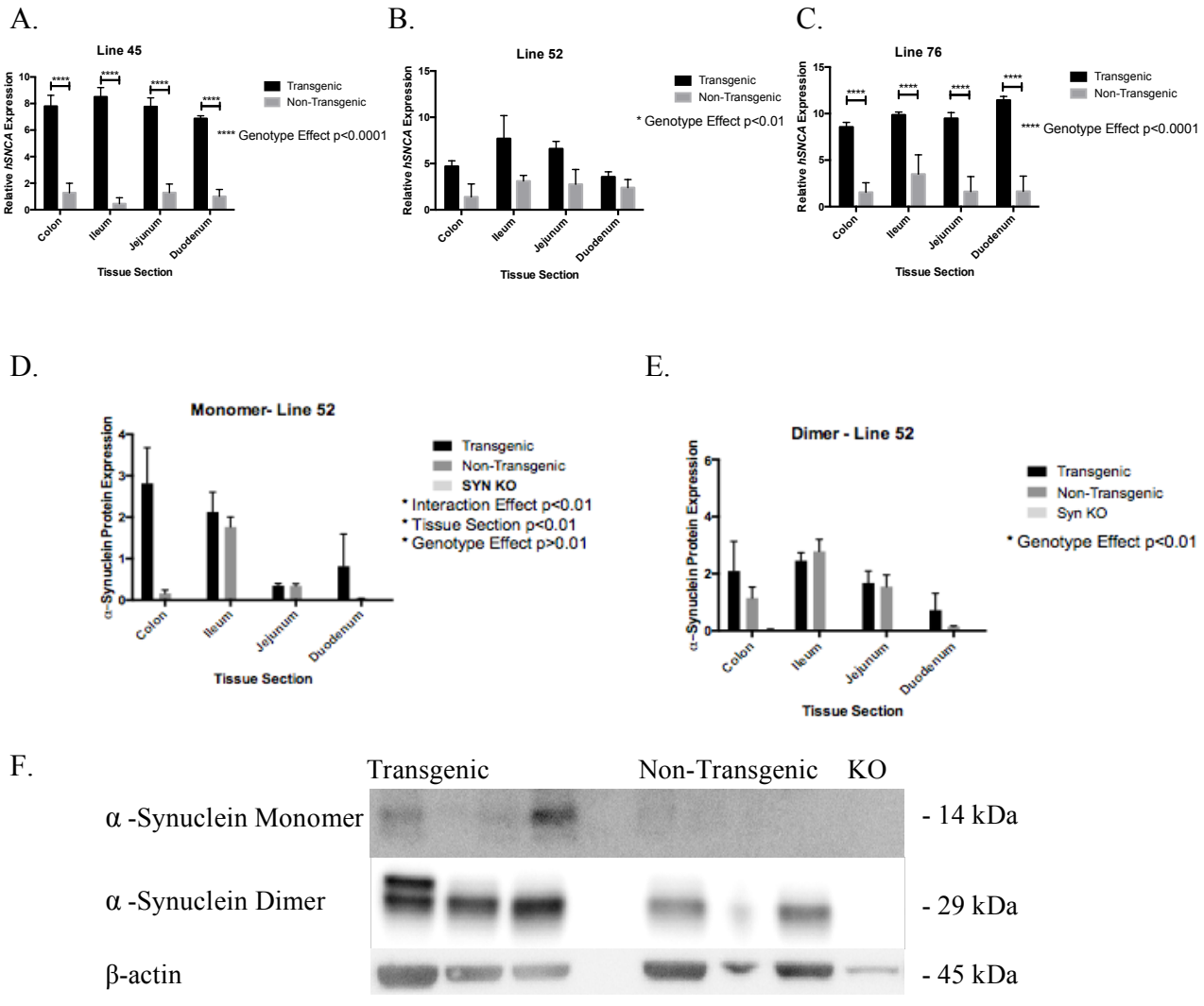

Figure 2: Human alpha-synuclein is produced in intestinal tissue of aged transgenic mice. qPCR analysis of intestinal tissue of 14-month-old Tg and NTg mice from **A)** Line 45, **B)** Line 53, and **C)** Line 76. Relative expression of hSNCA normalized to the average of two

housekeeping genes. hSNCA mRNA detected in small intestine and colon of Tg but not NTg mice. Significant effect of genotype ($p<0.01$) by two-way ANOVA. Western blot analysis of intestinal tissue of Tg and NTg mice, line 52, age 15 months. hSNCA **D)** monomer **(**14kDa) and **E)** dimer **(**26-28 kDa) levels normalized to levels of β-actin. Significant increase in hSNCA protein levels detected in small intestine and colon of Tg vs NTg mice. Tg, NTg, and one alpha-synuclein knockout (KO) sample were run on **F)** blot pictured. Significant effect of genotype, age, and interaction ($p<0.01$) by two-way ANOVA. n=4 Results shown are representative of 3 independent experiments.

We then confirmed the localization of hSNCA expression to enteric neurons using immunofluorescence microscopy. We stained intestinal sections with tyrosine hydroxylase (TH) and human alpha-synuclein (hSNCA) antibodies (Figure 3). We found hSNCA protein to be partially co-localized with TH in the Tg mice (Figure 3b,c), but there was no expression of hSNCA protein in the NTg mice (Figure 3a).

A. Line 52- NTg 40x Small Intestine

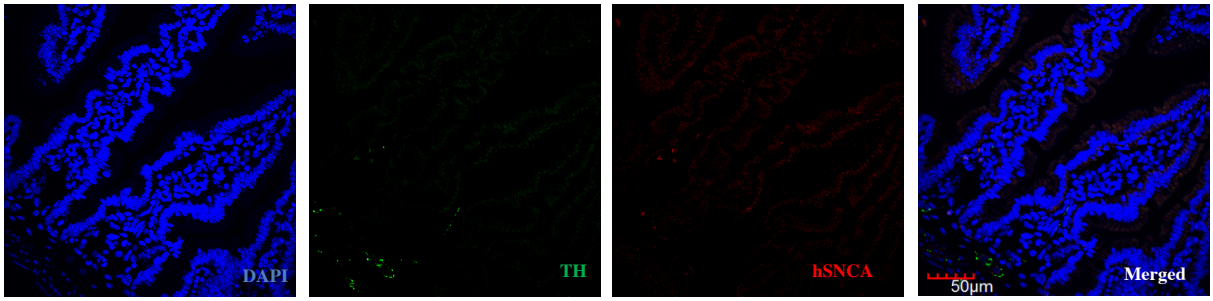

B. Line 45 Tg 40x Small Intestine

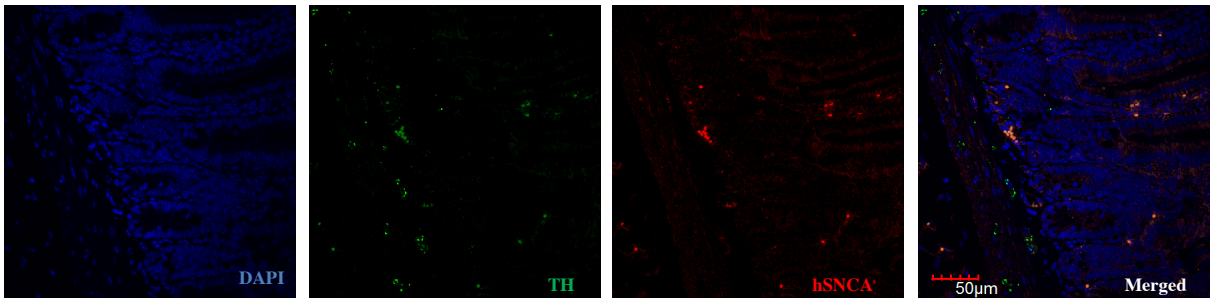

C. Line 45 Tg 60x Colon

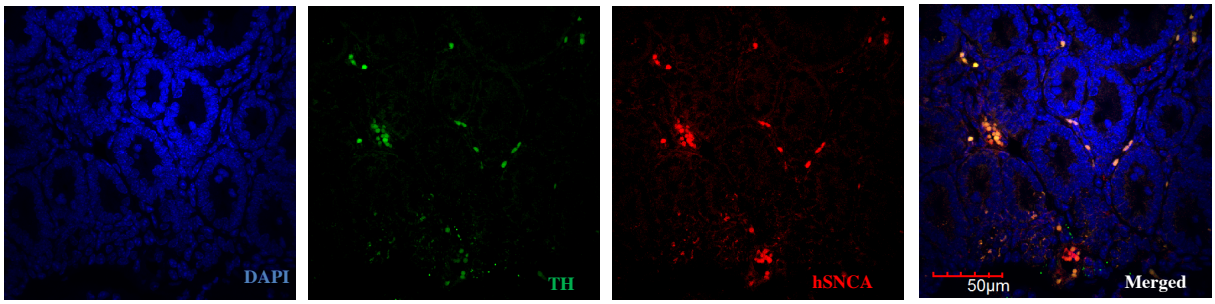

Figure 3: Human alpha-synuclein is localized to enteric neurons.
Confocal imaging of paraffin embedded sections **A)** NTg section at 40x, **B)** Tg section at 40x, and **C)** Tg section at 60x. hSNCA is stained for in the red channel, TH is in the green channel, and DAPI is in the blue channel. These images show hSNCA expression in Tg mice and not the NTg. Scale bar indicates 50 µm

Next, we compared the expression of hSNCA mRNA and protein in young versus aged line 45 mice. We found hSNCA mRNA to be expressed above background level in Tg young and aged mice (Figure 4a). hSNCA expression was highest in the colon, lowest in the duodenum and comparable in the jejunum and ileum (Figure 4a). We did not detect hSNCA protein in young Tg mice compared to NTg mice, despite evidence of transgene expression from qPCR data. We only detected hSNCA protein in aged Tg mice (Figure 4b). We detected two bands

when the blot was probed for hSNCA, which corresponded to the predicted molecular weights of the monomer and dimer of hSNCA protein. The dimer form was the primary form of the two, and therefore we analyzed levels of the dimer form of hSNCA protein at 29 kDa (Figure 4c). Dimerization of hSNCA is an important step in conformational transition and aggregation, and has also been found to accelerate the formation of neurotoxic aggregates and amyloid fibrils [35].

A.

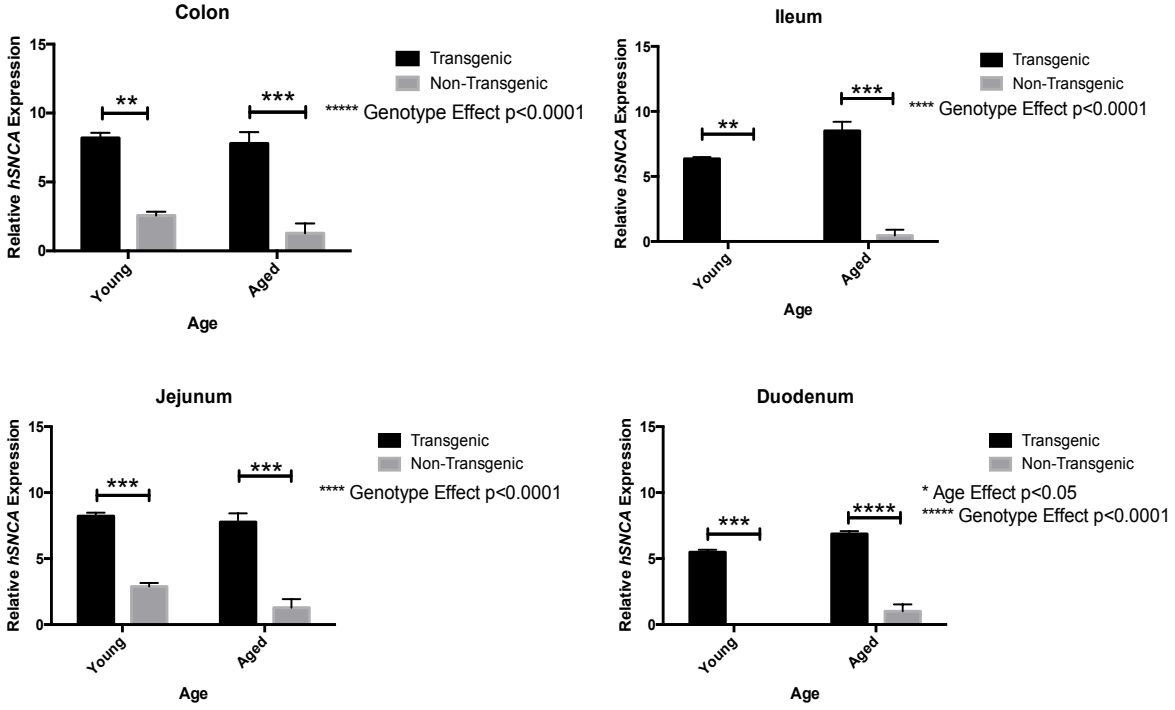

B.

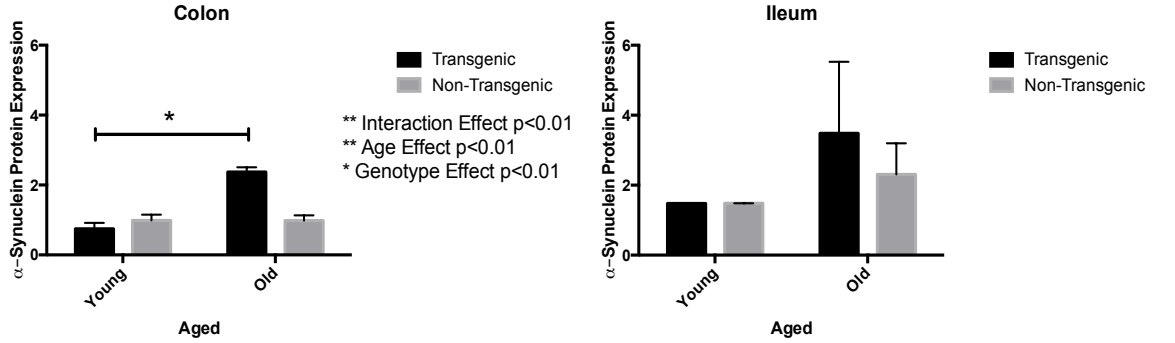

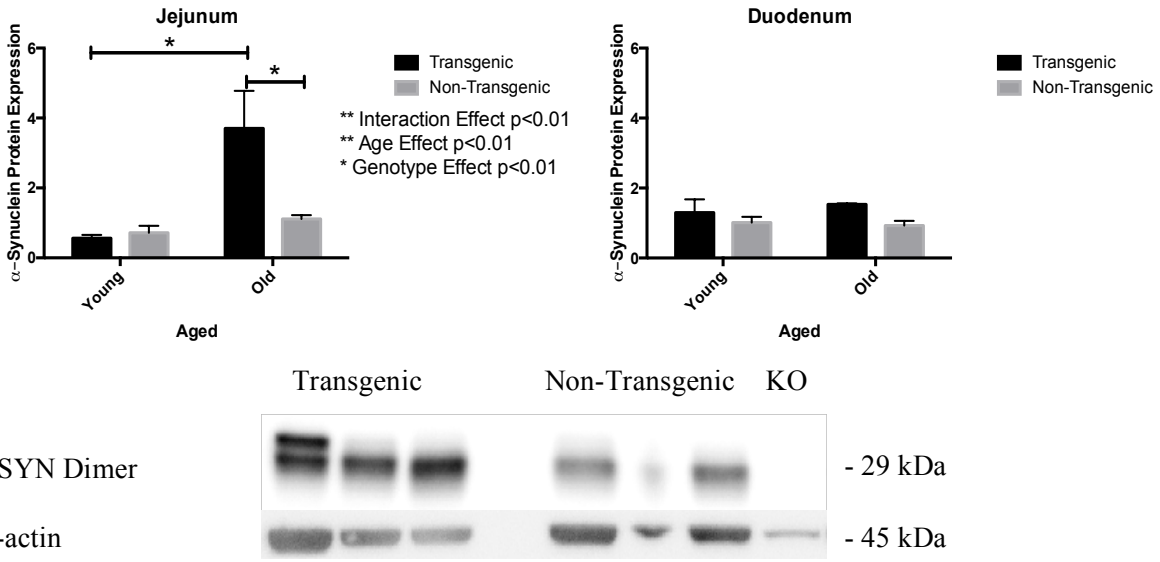

Figure 4: Human alpha-synuclein protein only accumulates in intestinal tissue of aged mice.
qPCR analysis of intestinal tissue from **A)** 14-month-old, line 45, Tg and NTg mice. Relative expression of hSNCA normalized to the average of two housekeeping genes Significant effect of genotype ($p<0.01$) by two-way ANOVA. n=3-4 **B)** Western Blot analysis of intestinal tissue from Tg and NTg line 45 mice age 15 months. Significant effect of genotype, age, and interaction ($p<0.01$) by two-way ANOVA. n=3-4. High molecular weight (29kDA), **C)** dimer form of hSNCA protein was analyzed. Results shown are representative of 7 independent experiments.

To see if the increased hSNCA in the Tg mice resulted in overt intestinal dysfunction, we conducted assays measuring intestinal motility. We found no differences in intestinal transit time between Tg and NTg or between young and aged mice (Figure 5a). We found no differences in fecal water content or fecal boli count between Tg and NTg aged line 45 mice (Figure 5b).

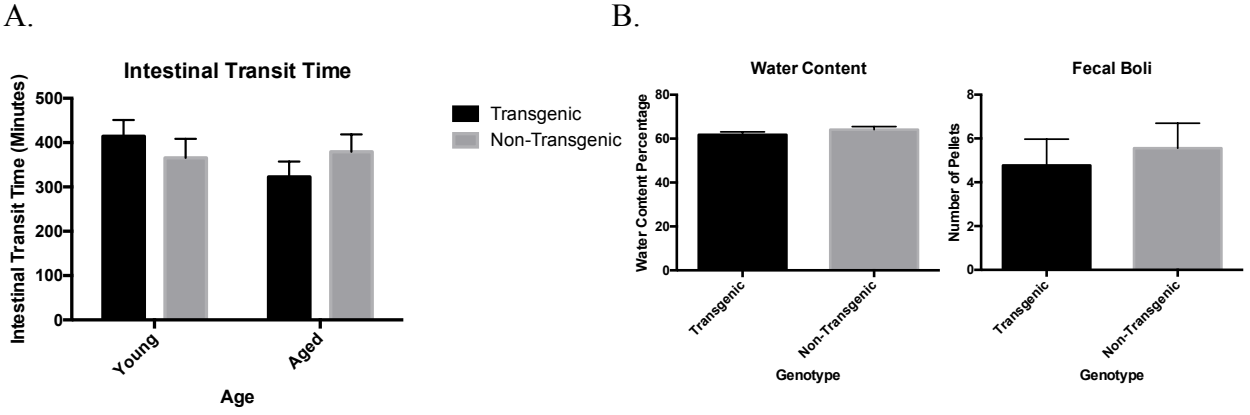

Figure 5: No changes in intestinal transit time, fecal water content, or fecal boli count. Aged line 45 and 76 mice were fasted for one hour and then gavaged with carmine red dye. The mice were placed in individual containers, and feces samples were collected. **A)** The time between gavage and expulsion of a red pellet was recorded. No significant difference found by two-way ANOVA. n=7-8 **B)** Aged line 76 mice were placed in separate containers for one hour and feces samples were collected and recorded immediately after defecation. Samples were weighed, dried overnight at 65°C and weighed again. Water content was calculated by percent change between wet and dry weight. No significant difference found by unpaired t-test. n= 8-11

To see if transgene expression resulted in a behavioral phenotype, we performed two assays to test for anxiety. We conducted an open field test and measured the amount of time to enter the center of the field. We found a significant difference in latency to enter the center in aged Tg mice (Figure 6a). Aged Tg mice required significantly more time to enter the center compared to NTg mice. We also conducted a marble-burying test as a measure of anxiety. We found that aged Tg mice buried significantly more marbles than NTg (Figure 6b). We found no differences between Tg and NTg young mice in the open field or marble-burying test.

A. Latency to Enter

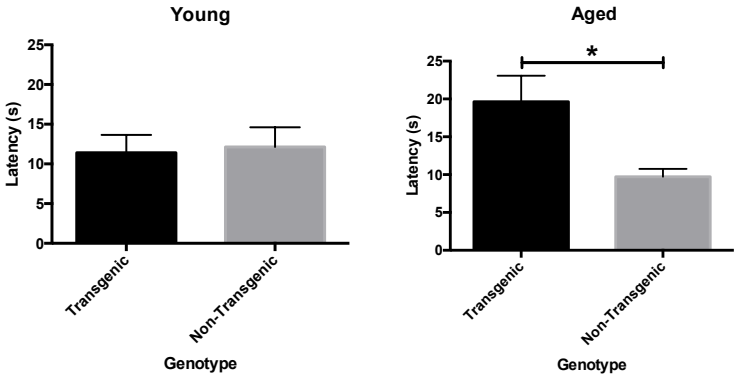

B. Marble Burying

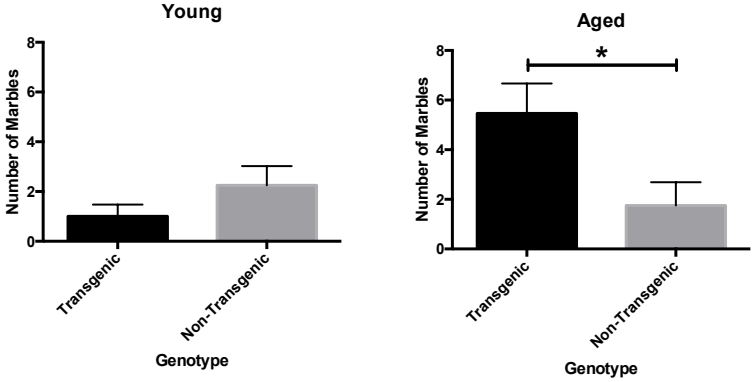

Figure 6: Human alpha-synuclein expression in transgenic mice results in age-dependent anxiety-like behavior.
Young and aged line 45 mice were placed in an open field. The amount of time it took to enter the center or the amount of time spent in an area was recorded. During an open field test **A)** Tg aged mice required significantly more time to enter the center as found by unpaired t-test, representative of anxiety-like behavior (n=5-11). Young and aged line 45 mice were placed in a container with 20 marbles. After 30 minutes, the number of marbles that were at least two-thirds buried in the bedding was recorded as buried by two observers blinded to genotype. During the marble burying assay **B)** Tg aged mice buried significantly more marbles as found by unpaired t-test, representative of anxiety-like behavior (n=8-12).

To see if the increased hSNCA in the Tg mice promoted intestinal inflammation, we evaluated the expression of a variety of cytokines by qPCR. We found significant differences by age in colon tissue for IL-6 (Figure 7a). We found significant differences by age, genotype and interaction in colon tissue for TGFβ (Figure 7b). We found no significant difference in expression of IL-6 and TGFβ in the small intestine (Figure a,b). We found no significant difference in expression of IL-10, TNF, or IL-1β in the small intestine and colon (Figure 7c,d,e).

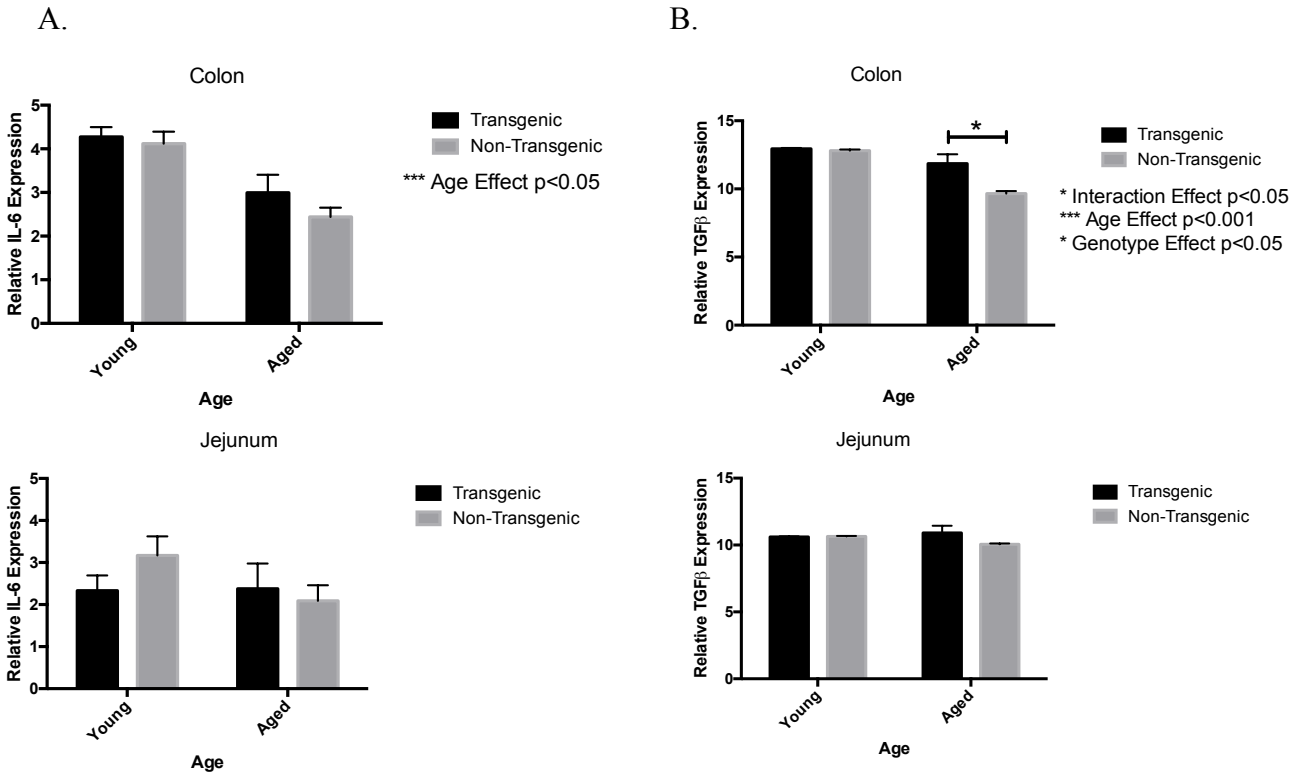

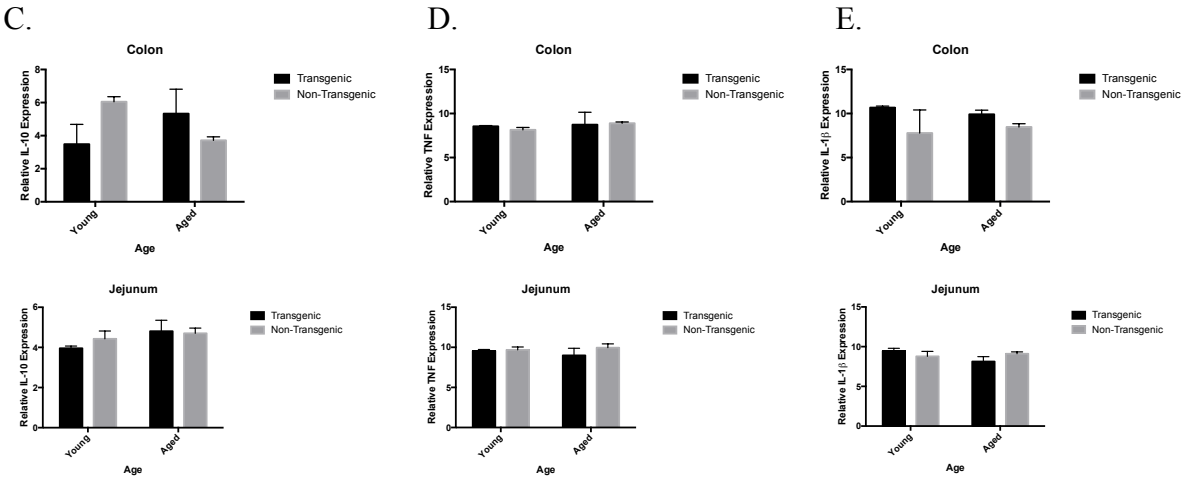

Figure 7: Age and genotype alter intestinal cytokine levels of IL-6 and TGFβ. qPCR analysis of intestinal tissue from 4 and14 month old, line 45, Tg and NTg mice. Relative expression of **A)** IL-6, **B)** TGFβ, **C)** IL-10, **D)** TNF, **E)** IL-1β normalized to the average of two housekeeping genes Significant effect of age in IL-6 and significant effect of interaction, age, and genotype in TGFβ in colon tissue ($p<0.05$) by two-way ANOVA Tukey's multiple comparisons test. n=3-4 No significant differences in cytokine mRNA levels in jejunum tissue of IL-6 and TGFβ, nor in colon and jejunum tissue of IL-10, TNF, and IL-1β by two-way ANOVA, Tukey's multiple comparisons test. n=3-4

In comparing mRNA expression of human alpha-synuclein we found no differences between males and females across qPCR analysis (Figure 8a), gastric motility analysis (Figure 8b), or behavioral analysis (Figure 8. Thus, for analysis purposes, data from males and females were combined. We continued to utilize approximately equal numbers of males and females in assays.

A. Sex Differences Across qPCR Data

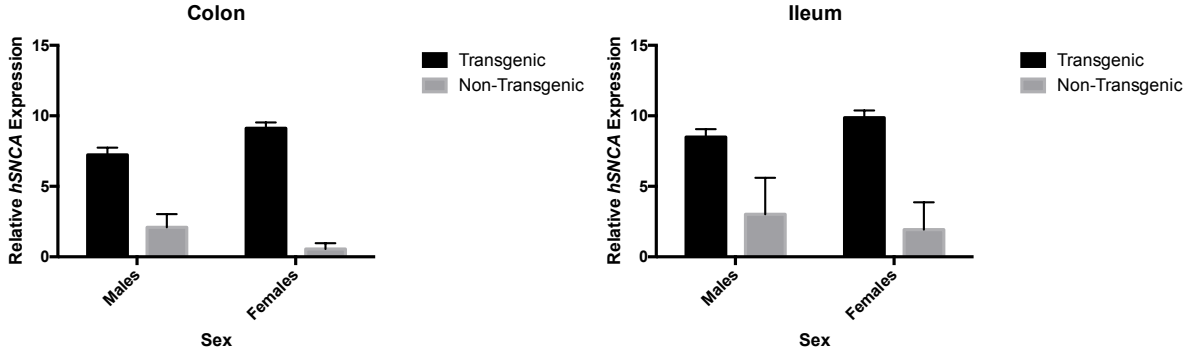

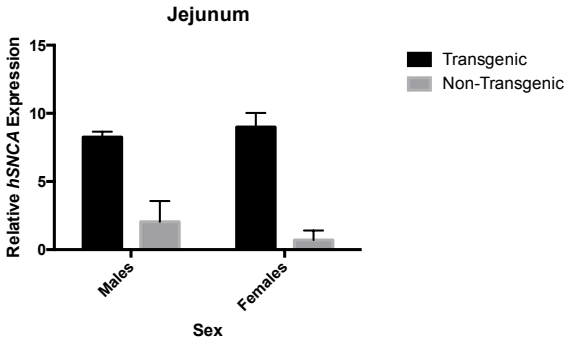

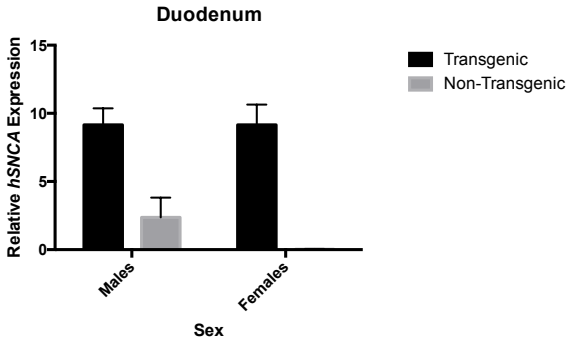

Sex Distribution for qPCR data

	Transgenic	Non-Transgenic
Males	4	4
Females	4	3

B. Sex Differences Across Gastric Motility Data

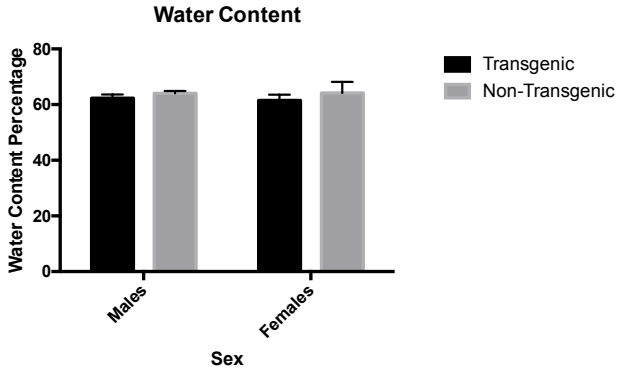

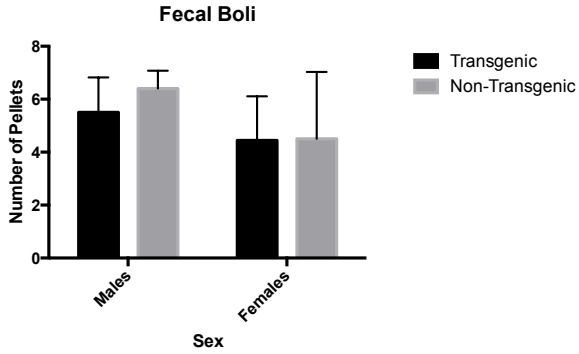

Sex Distribution for Gastric Motility Data

	Transgenic	Non-Transgenic
Males	4	5
Females	9	4

C. Sex Differences Across Behavioral Data

Latency to Enter Center

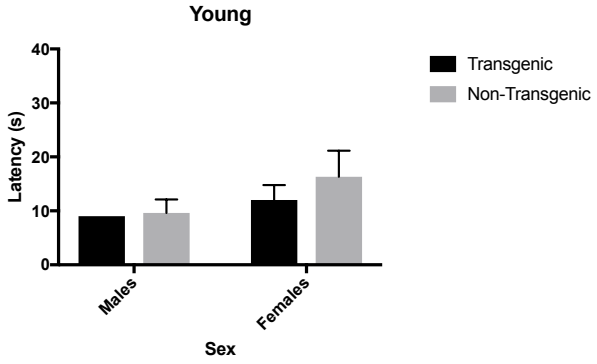

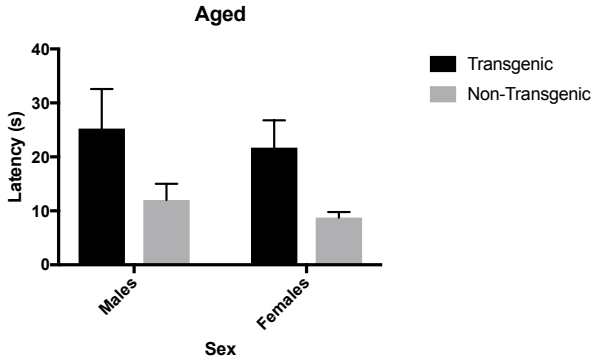

Marble Burying

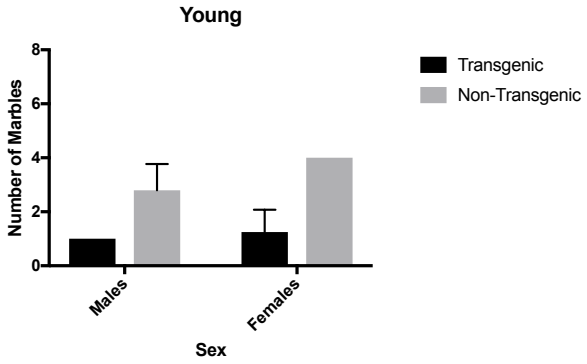

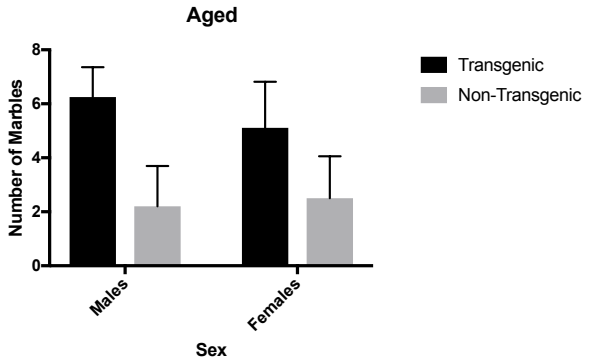

Sex Distribution for Young Behavioral Data

	Transgenic	Non-Transgenic
Males	1	5
Females	4	4

Sex Distribution for Aged Behavioral Data

	Transgenic	Non-Transgenic
Males	6	5
Females	9	4

Figure 8: No differences between sexes.
No differences between sex in **A)** qPCR analysis of hSNCA in intestinal tissue of young and aged Tg and NTg mice, **B)** gastric motility data from aged line 45 mice, and **C)** behavioral assays of young and aged Tg and NTg line 76 mice. No significant difference found by unpaired t-test. n corresponds to values in tables.

Discussion:

We confirmed that hSNCA is being expressed in the small intestine and colon of DBH-hSNCA mice. The amount being expressed varies based on the line and as such the number of copies of the transgene controlled by the DBH-BAC promoter. We determined that Line 45 and 76 had the highest expression of the transgene, and the rest of the experiments were conducted with those two lines. We found no differences between sexes in relative mRNA expression of human alpha-synuclein within each line. Based on the data, we decided to combine the sexes for the remaining experiments. We determined by immunohistochemistry that human alpha-synuclein is localized to enteric neurons in the small intestine and colon. The amount of mRNA expression remains the same between young and aged Tg mice; however, the amount of protein increases in aged Tg mice. This is an indication of protein accumulation in the aged Tg mice, possibly due to age-associated decreases in efficiency of proteostasis and/or clearance processes.

Previous studies have shown that phagocyte inefficiency is seen in PD and may be a reason that PD does not manifest until advanced age [36, 37]. In this study, we measured levels of the dimeric form of hSNCA. There is controversy as to which conformational form of hSNCA is normal and which is toxic [38]. Studies have shown that the dimeric form of hSNCA can accelerate the formation of neurotoxic aggregates and amyloid fibrils, which make up the characteristic Lewy bodies found in PD [35].

We did find a difference in the behavioral phenotype; aged Tg mice expressed an increase in anxiety-like behavior. This phenotype only manifested with age, which correlates to the accumulation of hSNCA protein in aged mice (Figure 4b). An increase in anxiety-like behavior is consistent with an increase in noradrenergic neurotransmission in the LC. Previous studies in animal models have shown that there is a peak in noradrenergic neurotransmission right before the degeneration of neurons in the LC [39-41]. In our PD model, we expect to have noradrenergic neurodegeneration in the LC preceding dopaminergic degeneration in the SNpc. However, according to our behavioral phenotype, we are seeing the opposite - an increase in noradrenergic neurotransmission. As PD pathology is an age-dependent, we could potentially see noradrenergic degeneration at an older time point. To determine if noradrenergic degeneration is occurring in the LC, we would need to directly measure norepinephrine levels. If we saw a decrease in norepinephrine in older mice, we would potentially see a loss of the anxiety-like behavior.

Another explanation for an increase in anxiety-like behavior may lie within the gut. Studies have shown that increased intestinal inflammation and permeability or altered gut microbiome can lead to anxiety-like behavior in mice [42, 43]. Anxiety has also been reported in inflammatory bowel disease [44, 45]. Multiple studies have linked inflammatory bowel disease

with an increased risk for PD [13, 46, 47]. The increased anxiety we see in the Tg mice may be an indicator of preliminary pathophysiology in the gut or due to altered norepinephrine levels. Gut pathophysiology and altered norepinephrine levels have both been implicated in the pathogenesis of PD.

We did find slight differences in cytokine markers in the aged Tg mice compared to NTg mice. We found a decrease in IL-6 and an increase in TGFβ in the colon of aged Tg mice compared to NTg. The differences we see in cytokine levels in aged mice and not young mice may be due to the accumulation of hSNCA protein we see in aged mice. The increase in hSNCA protein may be triggering a slight inflammatory response. IL-6 plays a variety of roles in the gut; it can promote inflammation and tight junction permeability, but it also induces repair [48-51]. IL-6 may promote permeability by modulation of tight junctions [50, 52] or by regulating immune cells that regulate tight junctions [51, 53]. IL-6 is also involved in intestinal epithelial proliferation and repair pathways [54]. A decrease in IL-6 may be due to decreased ability to repair injured epithelial layers and may lead to increased gut permeability. IL-6 could also limit gut permeability by altering epithelial cell homeostasis [55-58]. Additional assays would have to be conducted to determine the effect a change in IL-6 has on this mouse model. Furthermore, decreased mRNA levels of IL-6 may not indicate decreased protein levels of IL-6. In future experiments, it is also important for us to confirm protein expression of inflammatory cytokines by running a Multiplex ImmunoAssay (ELISA). Elevated levels of TGFβ are found in the cerebrospinal fluid of PD patients [59]. Increased levels of TGFβ in the gut can affect levels of TGFβ in cerebrospinal fluid via the vagus nerve [60]. TGFβ in previous mouse models has also been shown to activate microglia to prevent degeneration of neurons [61]. Upregulation of TGFβ precedes down regulation of proinflammatory cytokines [61]; this may be an additional indicator

that we are measuring pathology at a time point immediately preceding neurodegeneration. TGFβ may be acting as an anti-inflammatory cytokine to help balance any changes caused by an increase in hSNCA protein. Changes in cytokine levels and differences in inflammation between Tg and NTg mice may be more apparent after a challenge such as acute tissue injury through an animal model of experimental colitis.

We did not find evidence of overt gut pathophysiology in Tg mice. There was no difference in fecal boli counts, fecal water content, or intestinal transit time. At baseline, our model may not show phenotypic differences in gut pathophysiology, but perhaps in older (24+ month-old) mice or after a "second hit" with an environmental trigger, we may be able to detect synergy between hSNCA and an additional challenge factor and may find significant differences in intestinal transit time and gut permeability.

Overall, we know that genetically, the DBH-hSNCA mouse model resulted in successful expression of the hSNCA transgene. We detected expression and translation of hSNCA in the jejunum and colon. Although we did not detect the overt inflammation and gut pathophysiology we predicted, this may be induced through an environmental challenge or in older mice. PD is not a purely genetic disorder; rather it is multi-faceted and is affected by a variety of factors, including environmental triggers [62, 63]. Subjecting the DBH-hSNCA to an additional hit, such as a DSS challenge to induce colitis or an environmental toxin like a pesticide may be a more accurate representation of the of PD. Previous studies have also implicated a link between type 2 diabetes and sporadic PD [64-66]. PD and type 2 diabetes share dysregulated pathways [65]. These dysregulated pathways may generate enough inflammation to synergize with the genetic predisposition (the transgene) present in our model. For future studies, subjecting a cohort of mice to a high-fat-high-fructose (HFHF) diet to produce type-2 diabetes in aged mice, may foster

enough inflammation to promote alpha-synuclein phosphorylation and aggregation in the DBH-hSNCA mouse model [67].

For future studies, we plan to age an additional cohort of mice to 24+ months to see if we see a decrease in anxiety-like behavior indicative of neurodegeneration in the LC. We will also conduct an experiment with an acute or chronic colitis (DSS challenge) insult, comparing baseline and post-DSS measurements of weight, stool content, and peripheral immune cell populations as well as effects of DSS on central and peripheral nervous system function. We will also subject another cohort of mice to a HFHF diet to induce type-2-diabetes in aged mice, to evaluate how Tg mice respond to the dysregulated pathways involved in diabetes and PD compared to NTg mice. We will compare the levels of phosphorylated hSNCA and peripheral immune cell populations found in the gut of Tg mice in a HFHF diet and a control diet cohort. We plan to evaluate gut permeability by measuring FITC-dextran translocation from the gut lumen to the blood following oral gavage. In sum, the initial characterization that I have conducted of this new DBH-hSNCA mouse model has revealed new insights about how hSNCA is handled in the mammalian intestine and has laid the foundation for additional studies to be pursued by members of the Tansey lab.

References / Literature cited

[1] H. Braak, R.A. de Vos, J. Bohl, K. Del Tredici, Gastric alpha-synuclein immunoreactive inclusions in Meissner's and Auerbach's plexuses in cases staged for Parkinson's disease-related brain pathology, Neuroscience letters, 396 (2006) 67-72.

[2] K.M. Shannon, A. Keshavarzian, E. Mutlu, H.B. Dodiya, D. Daian, J.A. Jaglin, J.H. Kordower, Alpha-synuclein in colonic submucosa in early untreated Parkinson's disease, Movement disorders : official journal of the Movement Disorder Society, 27 (2012) 709-715.

[3] J.T. Bendor, T.P. Logan, R.H. Edwards, The function of alpha-synuclein, Neuron, 79 (2013) 1044-1066.

[4] J.P. Bach, U. Ziegler, G. Deuschl, R. Dodel, G. Doblhammer-Reiter, Projected numbers of people with movement disorders in the years 2030 and 2050, Movement disorders : official journal of the Movement Disorder Society, 26 (2011) 2286-2290.

[5] S.L. Kowal, T.M. Dall, R. Chakrabarti, M.V. Storm, A. Jain, The current and projected economic burden of Parkinson's disease in the United States, Movement disorders : official journal of the Movement Disorder Society, 28 (2013) 311-318.

[6] C. Klein, A. Westenberger, Genetics of Parkinson's disease, Cold Spring Harb Perspect Med, 2 (2012) a008888.

[7] R. Xia, Z.H. Mao, Progression of motor symptoms in Parkinson's disease, Neuroscience bulletin, 28 (2012) 39-48.

[8] E. Braak, D. Sandmann-Keil, U. Rub, W.P. Gai, R.A. de Vos, E.N. Steur, K. Arai, H. Braak, alpha-synuclein immunopositive Parkinson's disease-related inclusion bodies in lower brain stem nuclei, Acta neuropathologica, 101 (2001) 195-201.

[9] H. Chen, E.J. Zhao, W. Zhang, Y. Lu, R. Liu, X. Huang, A.J. Ciesielski-Jones, M.A. Justice, D.S. Cousins, S. Peddada, Meta-analyses on prevalence of selected Parkinson's nonmotor symptoms before and after diagnosis, Translational neurodegeneration, 4 (2015) 1.

[10] J. Dutkiewicz, S. Szlufik, M. Nieciecki, I. Charzynska, L. Krolicki, P. Smektala, A. Friedman, Small intestine dysfunction in Parkinson's disease, Journal of neural transmission (Vienna, Austria : 1996), 122 (2015) 1659-1661.

[11] M.G. Cersosimo, E.E. Benarroch, Pathological correlates of gastrointestinal dysfunction in Parkinson's disease, Neurobiology of disease, 46 (2012) 559-564.

[12] K.M. Shannon, A. Keshavarzian, H.B. Dodiya, S. Jakate, J.H. Kordower, Is alpha-synuclein in the colon a biomarker for premotor Parkinson's disease? Evidence from 3 cases, Movement disorders : official journal of the Movement Disorder Society, 27 (2012) 716-719.

[13] D. Hilton, M. Stephens, L. Kirk, P. Edwards, R. Potter, J. Zajicek, E. Broughton, H. Hagan, C. Carroll, Accumulation of alpha-synuclein in the bowel of patients in the pre-clinical phase of Parkinson's disease, Acta neuropathologica, 127 (2014) 235-241.

[14] G.A. Ferraro, F. De Francesco, C. Cataldo, F. Rossano, G. Nicoletti, F. D'Andrea, Synergistic effects of cryolipolysis and shock waves for noninvasive body contouring, Aesthetic Plast Surg, 36 (2012) 666-679.

[15] R. Sakakibara, T. Odaka, T. Uchiyama, M. Asahina, K. Yamaguchi, T. Yamaguchi, T. Yamanishi, T. Hattori, Colonic transit time and rectoanal videomanometry in Parkinson's disease, Journal of neurology, neurosurgery, and psychiatry, 74 (2003) 268-272.

[16] A. Gold, Z.T. Turkalp, D.G. Munoz, Enteric alpha-synuclein expression is increased in Parkinson's disease but not Alzheimer's disease, Movement disorders : official journal of the Movement Disorder Society, 28 (2013) 237-240.

[17] C.B. Forsyth, K.M. Shannon, J.H. Kordower, R.M. Voigt, M. Shaikh, J.A. Jaglin, J.D. Estes, H.B. Dodiya, A. Keshavarzian, Increased intestinal permeability correlates with sigmoid mucosa alpha-synuclein staining and endotoxin exposure markers in early Parkinson's disease, PloS one, 6 (2011) e28032.

[18] H. Pouclet, T. Lebouvier, E. Coron, S.B. des Varannes, T. Rouaud, M. Roy, M. Neunlist, P. Derkinderen, A comparison between rectal and colonic biopsies to detect Lewy pathology in Parkinson's disease, Neurobiology of disease, 45 (2012) 305-309.

[19] T.G. Beach, C.H. Adler, L.I. Sue, L. Vedders, L. Lue, C.L. White Iii, H. Akiyama, J.N. Caviness, H.A. Shill, M.N. Sabbagh, D.G. Walker, Multi-organ distribution of phosphorylated alpha-synuclein histopathology in subjects with Lewy body disorders, Acta neuropathologica, 119 (2010) 689-702.

[20] D.A. Hopkins, D. Bieger, J. deVente, W.M. Steinbusch, Vagal efferent projections: viscerotopy, neurochemistry and effects of vagotomy, Progress in brain research, 107 (1996) 79-96.

[21] C.J. Pomfrett, D.G. Glover, B.J. Pollard, The vagus nerve as a conduit for neuroinvasion, a diagnostic tool, and a therapeutic pathway for transmissible spongiform encephalopathies, including variant Creutzfeld Jacob disease, Medical hypotheses, 68 (2007) 1252-1257.

[22] S. Holmqvist, O. Chutna, L. Bousset, P. Aldrin-Kirk, W. Li, T. Bjorklund, Z.Y. Wang, L. Roybon, R. Melki, J.Y. Li, Direct evidence of Parkinson pathology spread from the gastrointestinal tract to the brain in rats, Acta neuropathologica, 128 (2014) 805-820.

[23] L.P. Kelly, P.M. Carvey, A. Keshavarzian, K.M. Shannon, M. Shaikh, R.A. Bakay, J.H. Kordower, Progression of intestinal permeability changes and alpha-synuclein expression in a mouse model of Parkinson's disease, Movement disorders : official journal of the Movement Disorder Society, 29 (2014) 999-1009.

[24] D. Lindqvist, E. Kaufman, L. Brundin, S. Hall, Y. Surova, O. Hansson, Non-motor symptoms in patients with Parkinson's disease - correlations with inflammatory cytokines in serum, PloS one, 7 (2012) e47387.

[25] A. Nicoletti, P. Fagone, G. Donzuso, K. Mangano, V. Dibilio, S. Caponnetto, K. Bendtzen, M. Zappia, F. Nicoletti, Parkinson's disease is associated with increased serum levels of macrophage migration inhibitory factor, Cytokine, 55 (2011) 165-167.

[26] P.M. Antony, N.J. Diederich, R. Balling, Parkinson's disease mouse models in translational research, Mammalian genome : official journal of the International Mammalian Genome Society, 22 (2011) 401-419.

[27] S.D. Robertson, N.W. Plummer, J. de Marchena, P. Jensen, Developmental origins of central norepinephrine neuron diversity, Nature neuroscience, 16 (2013) 1016-1023.

[28] K.C. Paul, J.S. Sinsheimer, S.L. Rhodes, M. Cockburn, J. Bronstein, B. Ritz, Organophosphate Pesticide Exposures, Nitric Oxide Synthase Gene Variants, and Gene-Pesticide Interactions in a Case-Control Study of Parkinson's Disease, California (USA), Environ Health Perspect, 124 (2016) 570-577.

[29] C. Naughton, D. O'Toole, D. Kirik, E. Dowd, Interaction between subclinical doses of the Parkinson's disease associated gene, alpha-synuclein, and the pesticide, rotenone, precipitates motor dysfunction and nigrostriatal neurodegeneration in rats, Behav Brain Res, 316 (2017) 160-168.

[30] V. Bellou, L. Belbasis, I. Tzoulaki, E. Evangelou, J.P. Ioannidis, Environmental risk factors and Parkinson's disease: An umbrella review of meta-analyses, Parkinsonism & related disorders, 23 (2016) 1-9.

[31] K. Xu, D.G. Di Luca, M. Orru, Y. Xu, J.F. Chen, M.A. Schwarzschild, Neuroprotection by caffeine in the MPTP model of parkinson's disease and its dependence on adenosine A2A receptors, Neuroscience, 322 (2016) 129-137.

[32] P. Bagga, A.B. Patel, Pretreatment of caffeine leads to partial neuroprotection in MPTP model of Parkinson's disease, Neural regeneration research, 11 (2016) 1750-1751.

[33] Y.H. Chuang, C.M. Lill, P.C. Lee, J. Hansen, C.F. Lassen, L. Bertram, N. Greene, J.S. Sinsheimer, B. Ritz, Gene-Environment Interaction in Parkinson's Disease: Coffee, ADORA2A, and CYP1A2, Neuroepidemiology, 47 (2016) 192-200.

[34] Y.A. Khadrawy, A.M. Salem, K.A. El-Shamy, E.K. Ahmed, N.N. Fadl, E.N. Hosny, Neuroprotective and Therapeutic Effect of Caffeine on the Rat Model of Parkinson's Disease Induced by Rotenone, Journal of dietary supplements, 14 (2017) 553-572.

[35] A. Roostaee, S. Beaudoin, A. Staskevicius, X. Roucou, Aggregation and neurotoxicity of recombinant alpha-synuclein aggregates initiated by dimerization, Mol Neurodegener, 8 (2013) 5.

[36] R.J. Phillips, C.N. Billingsley, T.L. Powley, Macrophages are unsuccessful in clearing aggregated alpha-synuclein from the gastrointestinal tract of healthy aged Fischer 344 rats, Anatomical record (Hoboken, N.J. : 2007), 296 (2013) 654-669.

[37] J.Y. Park, S.R. Paik, I. Jou, S.M. Park, Microglial phagocytosis is enhanced by monomeric alpha-synuclein, not aggregated alpha-synuclein: implications for Parkinson's disease, Glia, 56 (2008) 1215-1223.

[38] A. Deleersnijder, M. Gerard, Z. Debyser, V. Baekelandt, The remarkable conformational plasticity of alpha-synuclein: blessing or curse?, Trends Mol Med, 19 (2013) 368-377.

[39] K. Del Tredici, H. Braak, Dysfunction of the locus coeruleus-norepinephrine system and related circuitry in Parkinson's disease-related dementia, Journal of neurology, neurosurgery, and psychiatry, 84 (2013) 774-783.

[40] J.M. Fritschy, R. Grzanna, Restoration of ascending noradrenergic projections by residual locus coeruleus neurons: compensatory response to neurotoxin-induced cell death in the adult rat brain, J Comp Neurol, 321 (1992) 421-441.

[41] H. Hallman, G. Jonsson, Pharmacological modifications of the neurotoxic action of the noradrenaline neurotoxin DSP4 on central noradrenaline neurons, Eur J Pharmacol, 103 (1984) 269-278.

[42] M. Carabotti, A. Scirocco, M.A. Maselli, C. Severi, The gut-brain axis: interactions between enteric microbiota, central and enteric nervous systems, Annals of gastroenterology, 28 (2015) 203-209.

[43] M.L. Wong, A. Inserra, M.D. Lewis, C.A. Mastronardi, L. Leong, J. Choo, S. Kentish, P. Xie, M. Morrison, S.L. Wesselingh, G.B. Rogers, J. Licinio, Inflammasome signaling affects anxiety- and depressive-like behavior and gut microbiome composition, Molecular psychiatry, 21 (2016) 797-805.

[44] A.S. Bannaga, C.P. Selinger, Inflammatory bowel disease and anxiety: links, risks, and challenges faced, Clinical and experimental gastroenterology, 8 (2015) 111-117.

[45] L.A. Graff, J.R. Walker, C.N. Bernstein, Depression and anxiety in inflammatory bowel disease: a review of comorbidity and management, Inflammatory bowel diseases, 15 (2009) 1105-1118.

[46] S. Fujioka, S.E. Curry, K.D. Kennelly, P. Tacik, M.G. Heckman, Y. Tsuboi, A.J. Strongosky, J.A. van Gerpen, R.J. Uitti, O.A. Ross, T. Ikezu, Z.K. Wszolek, Occurrence of Crohn's disease with Parkinson's disease, Parkinsonism & related disorders, DOI 10.1016/j.parkreldis.2017.01.013(2017).

[47] J.C. Lin, C.S. Lin, C.W. Hsu, C.L. Lin, C.H. Kao, Association Between Parkinson's Disease and Inflammatory Bowel Disease: a Nationwide Taiwanese Retrospective Cohort Study, Inflammatory bowel diseases, 22 (2016) 1049-1055.

[48] S. Matsumoto, T. Hara, K. Mitsuyama, M. Yamamoto, O. Tsuruta, M. Sata, J. Scheller, S. Rose-John, S. Kado, T. Takada, Essential roles of IL-6 trans-signaling in colonic epithelial cells, induced by the IL-6/soluble-IL-6 receptor derived from lamina propria macrophages, on the development of colitis-associated premalignant cancer in a murine model, J Immunol, 184 (2010) 1543-1551.

[49] J. Mudter, M.F. Neurath, Il-6 signaling in inflammatory bowel disease: pathophysiological role and clinical relevance, Inflammatory bowel diseases, 13 (2007) 1016-1023.

[50] T. Suzuki, N. Yoshinaga, S. Tanabe, Interleukin-6 (IL-6) regulates claudin-2 expression and tight junction permeability in intestinal epithelium, J Biol Chem, 286 (2011) 31263-31271.

[51] S.J. Park, T. Nakagawa, H. Kitamura, T. Atsumi, H. Kamon, S. Sawa, D. Kamimura, N. Ueda, Y. Iwakura, K. Ishihara, M. Murakami, T. Hirano, IL-6 regulates in vivo dendritic cell differentiation through STAT3 activation, J Immunol, 173 (2004) 3844-3854.

[52] R. Al-Sadi, D. Ye, M. Boivin, S. Guo, M. Hashimi, L. Ereifej, T.Y. Ma, Interleukin-6 modulation of intestinal epithelial tight junction permeability is mediated by JNK pathway activation of claudin-2 gene, PloS one, 9 (2014) e85345.

[53] L. Zhou, Ivanov, II, R. Spolski, R. Min, K. Shenderov, T. Egawa, D.E. Levy, W.J. Leonard, D.R. Littman, IL-6 programs T(H)-17 cell differentiation by promoting sequential engagement of the IL-21 and IL-23 pathways, Nature immunology, 8 (2007) 967-974.

[54] K.A. Kuhn, N.A. Manieri, T.C. Liu, T.S. Stappenbeck, IL-6 stimulates intestinal epithelial proliferation and repair after injury, PloS one, 9 (2014) e114195.

[55] L.L. Healy, J.G. Cronin, I.M. Sheldon, Polarized Epithelial Cells Secrete Interleukin 6 Apically in the Bovine Endometrium, Biology of reproduction, 92 (2015) 151.

[56] S. Grivennikov, E. Karin, J. Terzic, D. Mucida, G.Y. Yu, S. Vallabhapurapu, J. Scheller, S. Rose-John, H. Cheroutre, L. Eckmann, M. Karin, IL-6 and Stat3 are required for survival of intestinal epithelial cells and development of colitis-associated cancer, Cancer cell, 15 (2009) 103-113.

[57] R. Bharti, G. Dey, M. Mandal, Cancer development, chemoresistance, epithelial to mesenchymal transition and stem cells: A snapshot of IL-6 mediated involvement, Cancer letters, 375 (2016) 51-61.

[58] Z.T. Schafer, J.S. Brugge, IL-6 involvement in epithelial cancers, The Journal of clinical investigation, 117 (2007) 3660-3663.

[59] M.P. Vawter, O. Dillon-Carter, W.W. Tourtellotte, P. Carvey, W.J. Freed, TGFbeta1 and TGFbeta2 concentrations are elevated in Parkinson's disease in ventricular cerebrospinal fluid, Exp Neurol, 142 (1996) 313-322.

[60] E. Ben-Menachem, A. Hamberger, T. Hedner, E.J. Hammond, B.M. Uthman, J. Slater, T. Treig, H. Stefan, R.E. Ramsay, J.F. Wernicke, et al., Effects of vagus nerve stimulation on amino acids and other metabolites in the CSF of patients with partial seizures, Epilepsy research, 20 (1995) 221-227.

[61] S.J. Haas, X. Zhou, V. Machado, A. Wree, K. Krieglstein, B. Spittau, Expression of Tgfbeta1 and Inflammatory Markers in the 6-hydroxydopamine Mouse Model of Parkinson's Disease, Front Mol Neurosci, 9 (2016) 7.

[62] S. Ghaisas, J. Maher, A. Kanthasamy, Gut microbiome in health and disease: Linking the microbiome-gut-brain axis and environmental factors in the pathogenesis of systemic and neurodegenerative diseases, Pharmacol Ther, 158 (2016) 52-62.

[63] K. Kieburtz, K.B. Wunderle, Parkinson's disease: evidence for environmental risk factors, Movement disorders : official journal of the Movement Disorder Society, 28 (2013) 8-13.

[64] J.A. Santiago, J.A. Potashkin, Shared dysregulated pathways lead to Parkinson's disease and diabetes, Trends in molecular medicine, 19 (2013) 176-186.

[65] J.A. Santiago, J.A. Potashkin, Integrative network analysis unveils convergent molecular pathways in Parkinson's disease and diabetes, PloS one, 8 (2013) e83940.

[66] J.A. Santiago, J.A. Potashkin, System-based approaches to decode the molecular links in Parkinson's disease and diabetes, Neurobiology of disease, 72 Pt A (2014) 84-91.

[67] M.E. de Sousa Rodrigues, M. Bekhbat, M.C. Houser, J. Chang, D.I. Walker, D.P. Jones, C.M. Oller do Nascimento, C.J. Barnum, M.G. Tansey, Chronic psychological stress and high-fat high-fructose diet disrupt metabolic and inflammatory gene networks in the brain, liver, and gut and promote behavioral deficits in mice, Brain, behavior, and immunity, 59 (2017) 158-172.